

Low-temperature Raman studies of sulfur-rich $\text{TlIn}(\text{S}_{1-x}\text{Se}_x)_2$ single crystals

Oleksandr O. Gomonnai^{a,b,*}, Michael Ludemann^c, Alexander V. Gomonnai^{a,d}, Ivan Yu. Roman^d, Alexander G. Slivka^a, Dietrich R.T. Zahn^c

^a Uzhhorod National University, 46 Pidhirna Str., 88000, Uzhhorod, Ukraine

^b Vlokh Institute of Physical Optics, 23 Dragomanov Str., 79005, Lviv, Ukraine

^c Semiconductor Physics, Chemnitz University of Technology, D-09107, Chemnitz, Germany

^d Institute of Electron Physics, Ukr. Nat. Acad. Sci., 21 Universytetska Str., 88017, Uzhhorod, Ukraine

ARTICLE INFO

Keywords:

Raman scattering
Layered crystals
Crystal disorder

ABSTRACT

Raman spectra of $\text{TlIn}(\text{S}_{1-x}\text{Se}_x)_2$ ($0 \leq x \leq 0.25$) single crystals in the frequency range 16–400 cm^{-1} were studied at $T = 30$ K in the $Z(\text{XX}+\text{XY})Z$ configuration. The experimental Raman spectra of $\text{TlIn}(\text{S}_{1-x}\text{Se}_x)_2$ single crystals were analyzed by multi-peak simulation by Lorentzian contours, enabling the peak frequencies, halfwidths and intensities to be determined. Their compositional dependences were studied. Compositional behaviour of Raman features revealed in the spectral regions 40–85 cm^{-1} and 190–220 cm^{-1} is discussed in view of different number of isoivalent S and Se atoms in structural groups corresponding to the general formula of $\text{In}_4\text{S}_{10-y}\text{Se}_y$.

1. Introduction

Solid solutions of chalcogenide-based ferroelectric single crystals attract a considerable scientific interest due to the existence of incommensurate modulated structures as well as polycritical points in the pressure–temperature (p, T) and composition–temperature (x, T) dependences [1,2]. Interesting objects for such studies are TIMX_2 -type crystals ($M = \text{Ga, In, X} = \text{Se, S}$) characterized by layered or chain-like structure. They were the first low-dimensional semiconductors, for which a series of phase transitions with modulated structures was discovered [3,4]. A special case is TlInS_2 , for which, based on experimental and theoretical studies, a sequence of phase transitions (PTs) as well as an incommensurate phase in the range of 190–220 K [3,4] and a complex (p, T) phase diagram are reported [5–9].

Note that the temperature behaviour of the dielectric constant in $\text{TlIn}(\text{S}_{1-x}\text{Se}_x)_2$ mixed crystals in the temperature interval including the phase transition range (190–216 K) showed that isoivalent anionic substitution of S by Se leads to a downward shift of the structural phase transition temperatures [10–12]. It was concluded that in the (x, T) phase diagram of the $\text{TlIn}(\text{S}_{1-x}\text{Se}_x)_2$ crystals a Lifshitz type point can exist at $x = 0.05$ [10]. However, other authors report contradictory data with respect to the phase transitions in $\text{TlIn}(\text{S}_{1-x}\text{Se}_x)_2$: substitution of S by Se only shifts the PTs, while neither narrowing of the incommensurate phase interval, nor Lifshitz type point is observed [11]. Therefore, in our opinion, all-round studies of sulfur-rich $\text{TlIn}(\text{S}_{1-x}\text{Se}_x)_2$ crystals using different techniques are important. In particular, we mean Raman spectroscopy which can provide additional information

regarding the lattice dynamics, compositional disorder and statistical character of chalcogen atom arrangement in the anion sublattice of these crystals.

Note that numerous publications by different authors were devoted to Raman scattering studies of TlInS_2 [5,13–21] and TlInSe_2 [22–24] crystals while only quite a few papers concerned $\text{TlIn}(\text{S}_{1-x}\text{Se}_x)_2$ solid solutions [25–28]. In the earliest study [25] the Raman scattering in $\text{TlIn}(\text{S}_{1-x}\text{Se}_x)_2$ was analyzed for a limited set of crystals ($x = 0.3, 0.5$ and 0.7) at room temperature with regard to the one-mode and two-mode compositional transformation of the phonon spectra with S \rightarrow Se substitution. The compositional dependence of the Raman-active mode frequencies and linewidths at room temperature was discussed for $\text{TlIn}(\text{S}_{1-x}\text{Se}_x)_2$ crystals with $x = 0, 0.25, 0.5$ and 0.75 [27,28].

Since, to our knowledge, low-temperature Raman studies of $\text{TlIn}(\text{S}_{1-x}\text{Se}_x)_2$ single crystals have not been reported so far, here we analyze the Raman features of their spectra in the compositional range of $0 \leq x \leq 0.25$ at $T = 30$ K.

2. Materials and methods

$\text{TlIn}(\text{S}_{1-x}\text{Se}_x)_2$ ($0 \leq x \leq 0.25$) single crystals were grown by the Bridgman technique [26,29]. The crystal quality and chemical composition were checked by methods described in Ref. [26]. The results of studies by X-ray diffraction, scanning electron microscopy and energy-dispersive X-ray spectroscopy obtained for the samples under investigation agree well with the data for the C_{2h}^6 space group, typical for TlInS_2 -type crystals at room temperature and atmospheric pressure [3,4].

* Corresponding author at: Uzhhorod National University, 46 Pidhirna Str., 88000, Uzhhorod, Ukraine.
E-mail address: oleksandr.gomonnai@uzhnu.edu.ua (O.O. Gomonnai).

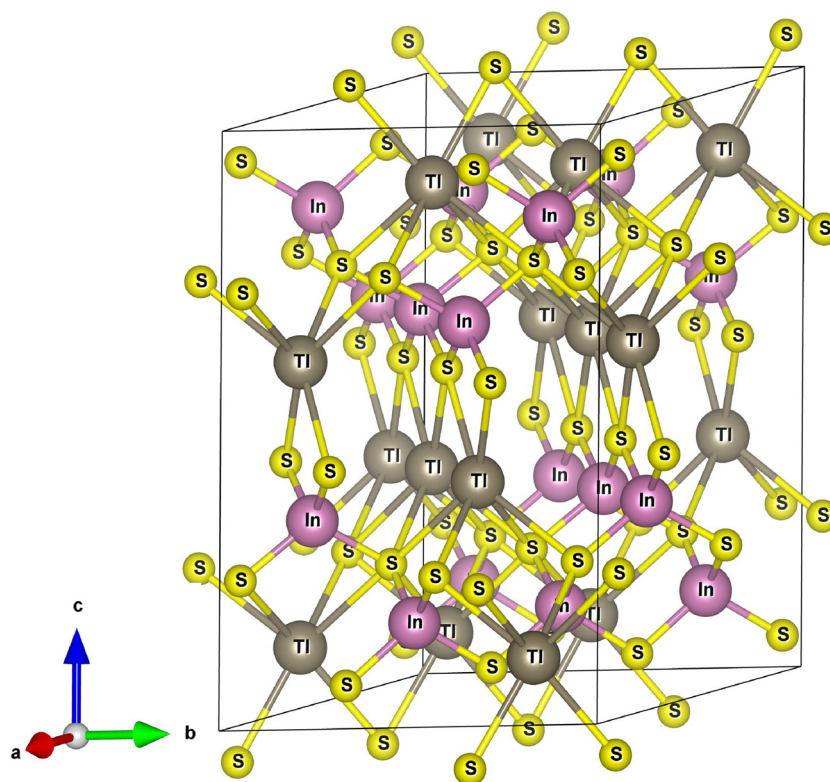


Fig. 1. Crystalline structure of monoclinic TlInS₂.

Raman measurements were performed using a Dilor XY 800 spectrometer equipped with a CCD camera. The instrumental resolution was in all cases better than 2 cm^{-1} . A Kr⁺ laser operating at 647.1 nm was used for excitation. As we could not define the X and Y axes unambiguously, the Raman spectra were measured in the Z(XX+XY)Z configuration with backscattering from the (001) plane. The samples were placed in a cryostat coupled to a temperature control system that is capable of stabilizing the sample temperature with an accuracy of $\pm 0.01\text{ K}$. We measured the spectra at certain steps with cooling from room temperature down to 30 K and, since we did not observe abrupt dramatical changes in the spectra, we believe that at least the Z axis did not change its direction with cooling.

3. Results and discussion

TlInS₂ is known to exist in various polytypes and structures, the most well known of them being described by C_{2h}^6 and D_{4h}^{18} space groups [3,4]. Fig. 1 shows the crystalline structure of monoclinic TlInS₂ built using the VESTA-3 software [30] based on the X-ray diffraction data [31]. TlInSe₂ crystal at room temperature has a chain-like tetragonal structure with D_{4h}^{18} symmetry group [32]. Detailed group-theoretical analyses of Raman-active vibrations in TlInS₂ were performed earlier [16,17]. According to the recent data, in the monoclinic C_{2h}^6 phase $10A_g + 14B_g$ Raman-active TlInS₂ modes exist at room temperature [21]. For the tetragonal TlInSe₂ crystal (D_{4h}^{18}), $1A_{1g} + 2A_{2g} + 2B_{2g} + 3E_g$ modes should exist in the Brillouin zone center [22].

Raman spectra of TlIn(S_{1-x}Se_x)₂ single crystals measured at 30 K are shown in Fig. 2. For TlInS₂ crystal we observed a total of 19 Raman peaks, their frequencies, shown in the figure, being generally in agreement with the earlier data [3,4,16,17,21].

The high-frequency maxima are usually assigned to internal vibrations of In₄S₁₀ tetrahedral structural units [14,16,17,21,26]. These tetrahedra are bonded by ionic-covalent bonds with Tl atoms located in the voids between them. The bands in the range 260–310 cm^{-1} correspond to In–S bond vibrations and the maxima at 310–360 cm^{-1} are

ascribed to the vibrations of S atoms. Lower-frequency bands correspond to translational vibrations of weaker van-der-Waals-type bonds between the In₄S₁₀ tetrahedra as well as bonds connecting Tl⁺ and InS₂⁻ ions [14,21]. A detailed analysis of the TlInS₂ translational modes (peak frequency assignment and force constant values) at room temperature was carried out in an earlier study [14].

Room-temperature Raman spectra of sulfur-rich TlIn(S_{1-x}Se_x)₂ single crystals with $x \leq 0.1$ were studied in our earlier paper devoted to the fabrication and characterization of these mixed crystals [26]. Here we present an intentional low-temperature Raman study performed at 30 K for an extended range of the mixed crystal compositions (up to $x = 0.25$) which enabled us to study the spectra in much more detail and to reveal vibrational modes which were not reported in the earlier publication [26]. Besides, the data of Ref [26], were limited to the spectral range above 45 cm^{-1} while here we analyze the spectral range down to 16 cm^{-1} which seems important in view of the role of low-frequency vibrational modes for phase transitions which are reported for TlInS₂ at 190–220 K [3,4] and can be predicted to shift towards lower temperatures with partial S → Se substitution.

The experimental low-temperature Raman spectra of TlIn(S_{1-x}Se_x)₂ single crystals were analyzed by multi-peak simulation by Lorentzian contours, enabling the peak frequencies, halfwidths and intensities to be determined. An example of such simulation for two spectral ranges for TlIn(S_{0.75}Se_{0.25})₂ is shown in Fig. 3.

As can be seen from Fig. 3a, for TlIn(S_{0.75}Se_{0.25})₂ the band structure in the range 35–70 cm^{-1} is complicated and the peak at $\omega = 38\text{ cm}^{-1}$ emerges from the contributions of two Lorentzian contours with the maxima at 38 cm^{-1} and 43 cm^{-1} . Similarly, the maximum at $\omega = 61\text{ cm}^{-1}$ is also described by two contours with the frequencies of 58 cm^{-1} at 61 cm^{-1} . Such approach to the analysis of the experimentally measured Raman spectra of TlIn(S_{1-x}Se_x)₂ single crystals with $x = 0, 0.01, 0.03, 0.05, 0.08, 0.1, 0.15$ and 0.25 at 30 K enabled us to analyze the compositional dependences of the band halfwidths (examples are shown in Fig. 4) and to build compositional dependences of the optical phonon frequencies (Fig. 5). Note that the multi-peak fitting

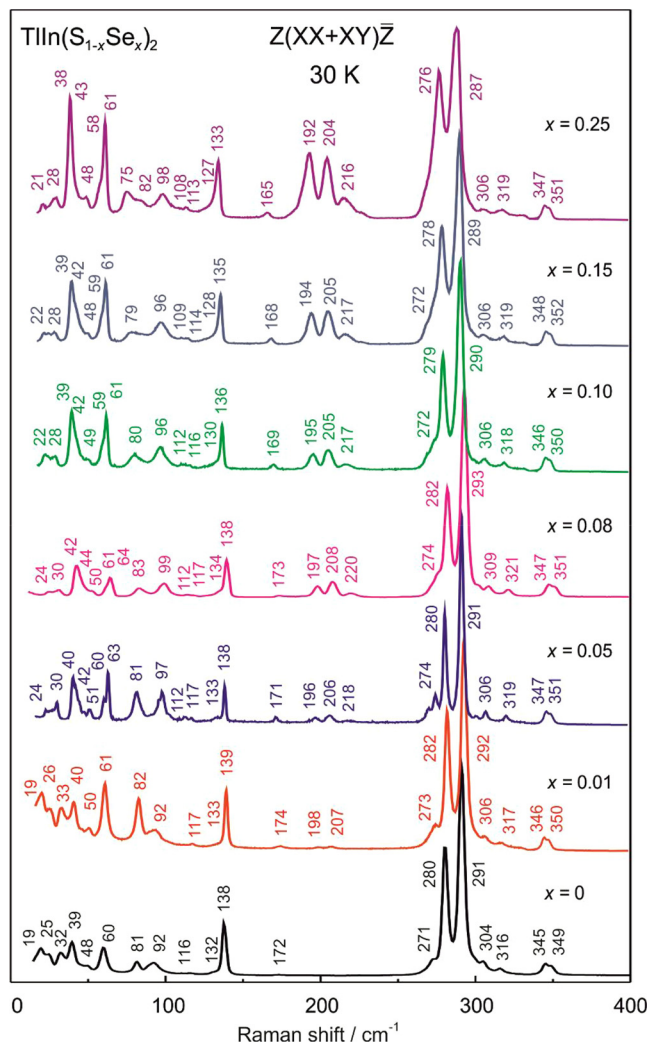


Fig. 2. Raman spectra of sulfur-rich $\text{TlIn}(\text{S}_{1-x}\text{Se}_x)_2$ single crystals in the $Z(\text{XX}+\text{XY})\bar{Z}$ configuration at the temperature of 30 K.

procedure was not performed in our earlier study at room temperature [26]; moreover, in the present case the fitting is definitely more efficient due to the better signal-to-noise ratio in comparison with the room-temperature data [26] and to the vibrational peak narrowing at lower temperatures.

Analysis of the compositional dependences of optical mode bandwidths for different spectral ranges shows that they have a trend to

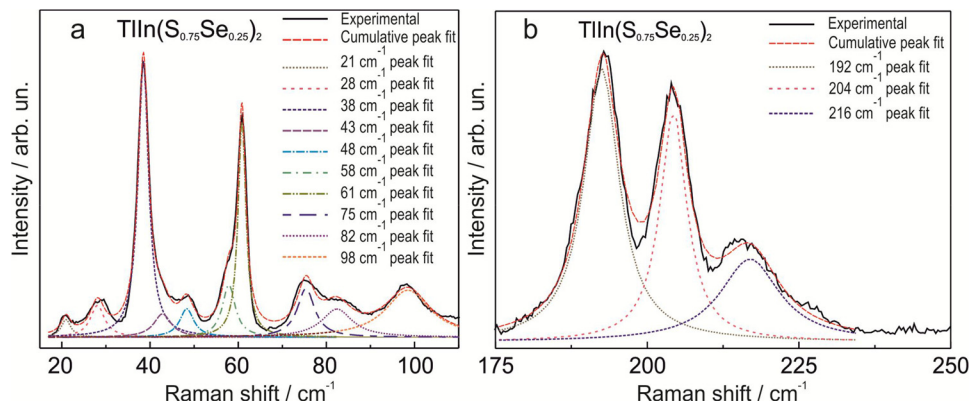


Fig. 3. Raman spectra of $\text{TlIn}(\text{S}_{0.75}\text{Se}_{0.25})_2$ single crystal in the $Z(\text{XX}+\text{XY})\bar{Z}$ configuration in the ranges of 17–120 cm^{-1} (a) and 175–250 cm^{-1} (b) at 30 K and their multi-peak Lorentzian simulation.

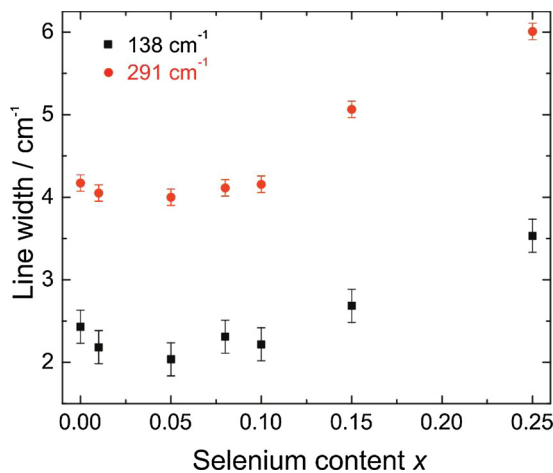


Fig. 4. Dependence of the full width at half maximum for the Raman peaks of sulfur-rich $\text{TlIn}(\text{S}_{1-x}\text{Se}_x)_2$ single crystals at 138 and 291 cm^{-1} on the selenium content at the temperature of 30 K.

increase with selenium content at $x \geq 0.1$. Note that a similar analysis was performed earlier for the high-frequency bands (250–350 cm^{-1}) for $\text{TlIn}(\text{S}_{1-x}\text{Se}_x)_2$ single crystals ($x = 0, 0.25, 0.5, 0.75$) at room temperature [27,28]. It showed a maximum in the compositional dependence of the high-frequency mode bandwidths to be reached at $x = 0.5$ corresponding to the maximal disorder in the solid solutions. Our data for $\text{TlIn}(\text{S}_{0.75}\text{Se}_{0.25})_2$ show noticeably lower Raman bandwidths for the high-frequency range compared to Refs [27,28], since our measurements were carried out at a much lower temperature (30 K).

Figs. 2 and 5 shows that with increasing selenium content in $\text{TlIn}(\text{S}_{1-x}\text{Se}_x)_2$ single crystals a decrease of frequency is observed for all bands except for the one at 93 cm^{-1} . Besides, new bands appear both in the low-frequency range of 30–90 cm^{-1} and in the range of 190–220 cm^{-1} .

In the low-frequency range the band at 19 cm^{-1} is revealed in the spectra of TlInS_2 and $\text{TlIn}(\text{S}_{0.99}\text{Se}_{0.01})_2$ while with further increasing Se content it is no longer observed because of its probably decreasing frequency. At $x = 0.03$ a new Raman band at $\omega = 64 \text{ cm}^{-1}$ is observed, an additional peak at $\omega = 42 \text{ cm}^{-1}$ is revealed at $x = 0.05$ while at $x = 0.25$ we recorded a new maximum at $\omega = 82 \text{ cm}^{-1}$. As noted earlier [14], this range corresponds to the bands related to the vibrations of Tl^+ ions and $\text{In}_4^3 + \text{S}_{10}^{2-}$ units and rigid-layer vibrations. The above mentioned compositional variation of this part of the $\text{TlIn}(\text{S}_{1-x}\text{Se}_x)_2$ single crystal Raman spectra is related to the appearance of $\text{In}_4^3 + \text{S}_{10}^{2-}$ structural groups or, more likely, more complex $\text{In}_4\text{S}_{10-y}\text{Se}_y$ units.

A slight downward shift of an intermediate-frequency band from

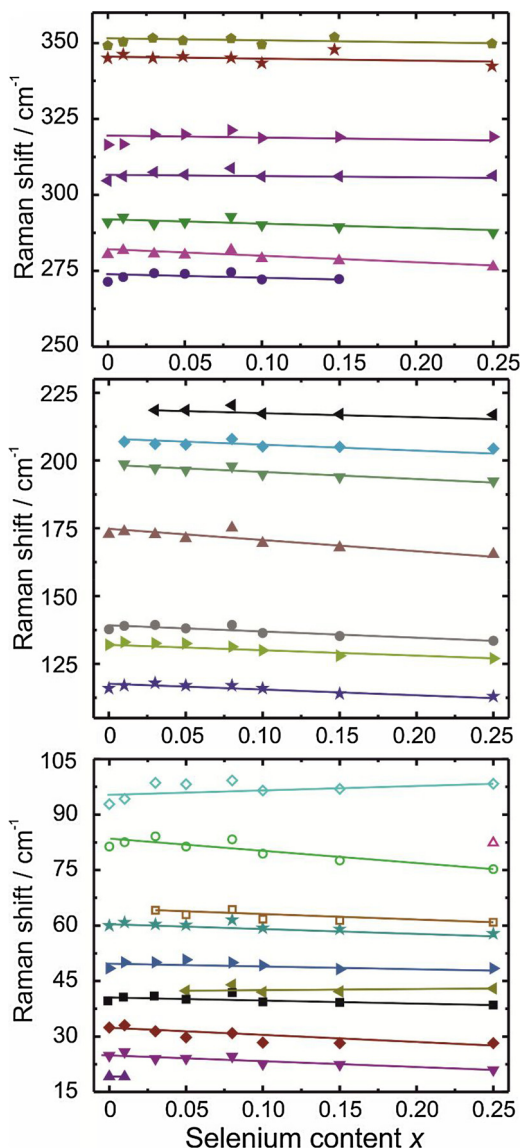


Fig. 5. Dependence of Raman line frequencies for sulfur-rich $\text{TlIn}(\text{S}_{1-x}\text{Se}_x)_2$ single crystals at the temperature of 30 K on the selenium content.

138 to 133 cm^{-1} is in agreement with the one-mode behaviour, typical for vibrations, external with respect to the pronounced structural units (in this case – In_4S_{10} tetrahedra).

For $\text{TlIn}(\text{S}_{1-x}\text{Se}_x)_2$ solid solutions even for quite small (1%) selenium

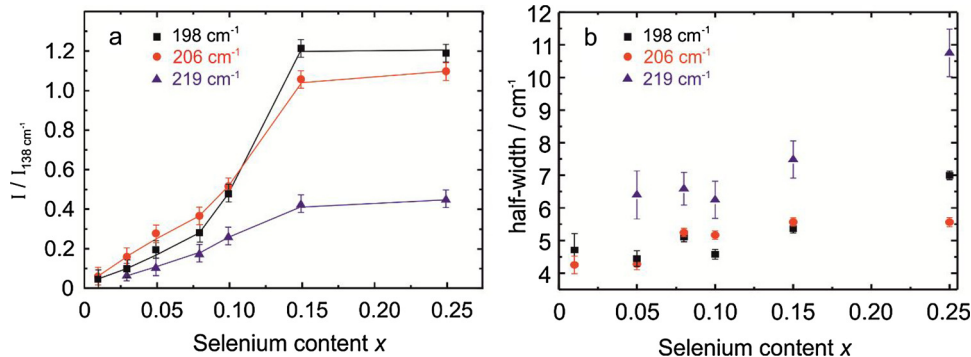


Fig. 6. Dependence of the normalized intensities (a) and halfwidths (b) of the Raman peaks at 198, 206 and 219 cm^{-1} on the selenium content x in $\text{TlIn}(\text{S}_{1-x}\text{Se}_x)_2$ crystals.

content new bands appear near 198 and 207 cm^{-1} (Fig. 2). With increasing x the bands at 198 and 207 cm^{-1} are revealed more distinctly while at $x = 0.03$ a maximum at $\omega = 219 \text{ cm}^{-1}$ appears. The compositional behaviour of the intensities of the Raman peaks at 198, 207 and 219 cm^{-1} normalized by the intensity of the one at 138 cm^{-1} is shown in Fig. 6a. Fig. 6b illustrates the behaviour of their halfwidths. As can be seen from the figure, the intensities of the Raman peaks at 198, 207 and 219 cm^{-1} increases with the selenium content and for $\text{TlIn}(\text{S}_{0.75}\text{Se}_{0.25})_2$ the lowest-frequency peak of this group becomes the most intense (Fig. 3b). The frequency positions tend to decrease with Se content (Figs. 2 and 4) while the band halfwidths increase. Note that the highest-frequency peak practically does not shift at all, while its essential broadening is observed.

In the high-frequency range 250–350 cm^{-1} (Fig. 5) of $\text{TlIn}(\text{S}_{1-x}\text{Se}_x)_2$ Raman spectra the S \rightarrow Se substitution results in a slight decrease of the high-energy band frequencies at 280, 291 and 345 cm^{-1} corresponding to the internal vibrations of the In_4S_{10} tetrahedra.

As noted above, the earlier studies [27,28] of $\text{TlIn}(\text{S}_{1-x}\text{Se}_x)_2$ single crystals ($x = 0, 0.25, 0.5, 0.75, 1$) at room temperature were devoted to the high-frequency (250–360 cm^{-1}) spectral range of the Raman spectra. The authors observed the increasing Se content to result in a downward shift of the maxima as well as their broadening. However, in Refs [27,28] there is no notice of any additional features in the range of 200 cm^{-1} . Bands appearing in the range of 200 cm^{-1} were reported for $\text{TlIn}(\text{S}_{1-x}\text{Se}_x)_2$ single crystals with $x = 0.3, 0.5, 0.7$ [25], but no detailed analysis of the compositional dependence of their characteristics (frequencies, halfwidths and intensities) was presented.

One should expect a two-mode behaviour for the high-frequency internal vibrations of pronounced structural units in the Raman of spectra of $\text{TlIn}(\text{S}_{1-x}\text{Se}_x)_2$ crystals. From this point of view, the peaks observed in the mixed crystal spectra in the range of 190–220 cm^{-1} could be ascribed to the vibrations of $\text{In}_4\text{Se}_{10}$ type tetrahedra similar to the In_4S_{10} tetrahedra in TlInS_2 responsible for the peaks at 280 and 291 cm^{-1} . However, Fig. 7 shows that for TlInSe_2 the Raman spectra measured at 30 K exhibit similar intense peaks at 177 and 189 cm^{-1} , which is noticeably below the frequencies of the peaks observed in the mixed crystal spectra. In spite of a clear qualitative agreement with the predictions of the two-mode behaviour, quantitatively the assignment of the peaks in the range of 190–220 cm^{-1} to the vibrations of $\text{In}_4\text{Se}_{10}$ tetrahedra does not seem reasonable.

In our opinion, in this case the situation is more complicated since in $\text{TlIn}(\text{S}_{1-x}\text{Se}_x)_2$ mixed crystals the pronounced structural groups of $\text{In}_4\text{S}(\text{Se})_{10}$ type can contain different number of isovalent S and Se atoms corresponding to the general formula $\text{In}_4\text{S}_{10-y}\text{Se}_y$ where y is an integer from 1 to 9. For sulfur-rich $\text{TlIn}(\text{S}_{1-x}\text{Se}_x)_2$ compounds the probability of formation of pure $\text{In}_4\text{Se}_{10}$ tetrahedra is far below the corresponding probabilities for the “mixed” $\text{In}_4\text{S}_{10-y}\text{Se}_y$ units. Still, the probability of the existence of In_4S_{10} tetrahedra for $x \leq 0.25$ is quite

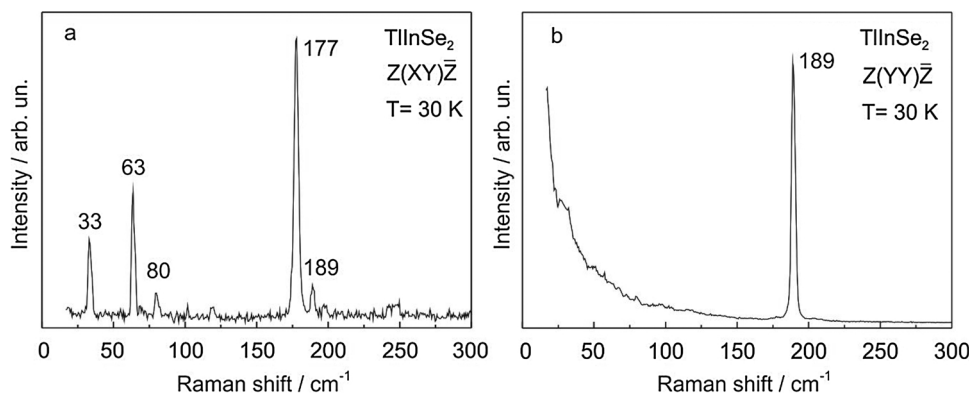


Fig. 7. Raman spectra at 30 K of TlInSe₂ single crystal in the Z(XY) \bar{Z} (a) and Z(YY) \bar{Z} (b) scattering configurations excited by a 514.5 nm line of Ar⁺ laser.

high that is clearly confirmed by the measured spectra (Fig. 2). Hence, it is reasonable to relate the bands observed in the range of 190–220 cm⁻¹ to the vibrations of In₄S_{10-y}Se_y tetrahedra in the structure of the mixed TlIn(S_{1-x}Se_x)₂ crystals. The contribution of structural groups with different *y* values is responsible for the bands at 190–220 cm⁻¹ being noticeably broader than the peaks corresponding to the vibrations of In₄S₁₀ tetrahedra for TlInS₂ (the bottom curve in Fig. 2) and In₄Se₁₀ tetrahedra for TlInSe₂ (Fig. 7).

4. Conclusions

Low-temperature (30 K) Raman spectra of TlIn(S_{1-x}Se_x)₂ (0 ≤ *x* ≤ 0.25) single crystals in the frequency range 16–400 cm⁻¹ were measured in the Z(XX+XY) \bar{Z} configuration. The spectra were analyzed by multi-peak Lorentzian simulations. Compositional dependences of the Raman peak positions, normalized intensities and halfwidths at *T* = 30 K were plotted.

TlIn(S_{1-x}Se_x)₂ Raman bands in the lower-frequency range ($\omega < 175$ cm⁻¹) mostly exhibit a typical one-mode compositional behaviour with a slight frequency shift. Still, with increasing selenium content new bands emerge in this frequency range near 42, 64, and 82 cm⁻¹ which is the evidence for a more complicated transformation of the vibrational spectrum, most likely related to the vibrations of bonds connecting Tl atoms to InS(Se)₂ units.

Raman bands appearing in the mixed crystal spectra in the higher-frequency range (190–220 cm⁻¹) are most likely related not to the vibrations of In₄Se₁₀ tetrahedra (as one should expect for a two-mode behaviour, typical for pronounced structural units in compound crystals), but rather to In₄S(Se)₁₀ with variable chalcogen ratio, for which the probability of formation in sulfur-rich TlIn(S_{1-x}Se_x)₂ mixed crystals is much higher.

Acknowledgements

O.O. Gomonnai gratefully acknowledges Deutscher Akademischer Austauschdienst (DAAD, project No. A/12/85971) for the financial support of his research at Chemnitz University of Technology. The authors are grateful to Yu.M. Azhniuk for helpful discussion.

References

- [1] O. Andersson, O. Chobal, I. Rizak, V. Rizak, *Phys. Rev. B* 80 (2009) 174107/1-5.
- [2] K.Z. Rushchanskii, A. Molnar, R. Bilanych, R. Yevych, A. Kohutyeh,

- Yu.M. Vysochanskii, V. Samulionis, J. Banys, *Phys. Rev. B* 93 (2016) 014101/1-12.
- [3] K.R. Allakhverdiev, T.G. Mamedov, B. Akmoğlu, S.S. Ellialtıoğlu, *Turk. J. Phys.* 18 (1994) 1–66.
- [4] A.M. Panich, *J. Phys.: Condens. Matter.* 20 (2008) 293202/1-42.
- [5] W. Henkel, H.D. Hochheimer, C. Carlone, A. Werner, S. Ves, H.G. Schnering, *Phys. Rev. B* 26 (1982) 3211–3221.
- [6] K.R. Allakhverdiev, T.G. Mamedov, G.I. Peresada, E.G. Ponatovski, Ya.N. Sharifov, *Sov. Phys. Solid State* 27 (1985) 568–569.
- [7] E. Bairamova, K.R. Allakhverdiev, B.G. Akinoglu, T. Arai, T.G. Mamedov, *Turk. J. Phys.* 18 (1994) 497–506.
- [8] O.O. Gomonnai, P.P. Guranich, M.Yu. Rigan, I.Yu. Roman, A.G. Slivka, *High Press. Res.* 28 (2008) 615–619.
- [9] P.P. Guranich, R.R. Rosul, O.O. Gomonnai, A.G. Slivka, I.Yu. Roman, A.V. Gomonnai, *Solid State Commun.* 106 (2014) 21–24.
- [10] M.Yu. Seyidov, R.A. Suleymanov, F. Salehli, *Phys. Scr.* 84 (2011) 015601.
- [11] A.U. Sheleg, V.G. Hurtavy, V.V. Shautsova, V.A. Aliev, *Phys. Solid State* 54 (2012) 622–625.
- [12] R.R. Rosul, P.P. Guranich, O.O. Gomonnai, A.G. Slivka, M. Yu Rigan, V.M. Rubish, O.G. Guranich, A.V. Gomonnai, *Semicond. Phys. Quant. Electron. Optoelectron.* 15 (2012) 35–37.
- [13] N.M. Gasanly, B.N. Mavrin, K.E. Sterin, V.I. Tagirov, Z.D. Khalafov, *Phys. Status Solidi B* 86 (1978) K49–K53.
- [14] N.M. Gasanly, A.F. Goncharov, N.N. Melnik, A.S. Ragimov, V.I. Tagirov, *Phys. Status Solidi B* 116 (1983) 427–443.
- [15] M. Isik, N.M. Gasanly, F. Korkmaz, *Phys. B: Condens. Matter* 421 (2013) 50–52.
- [16] V.M. Burlakov, A.P. Ryabov, M.P. Yakheev, E.A. Vinogradov, N.N. Melnik, N.M. Gasanly, *Phys. Status Solidi B* 153 (1989) 727–739.
- [17] K.R. Allakhverdiev, S.S. Babaev, M.M. Tagiev, M.M. Shirinov, *Phys. Status Solidi B* 152 (1989) 317–327.
- [18] R. Paucar, K. Harada, R. Matsumoto, K. Wakita, Y.G. Shim, O. Alekperov, N. Mamedov, *Phys. Status Solidi C* 10 (2013) 1132–1135.
- [19] R. Paucar, Y.G. Shim, K. Wakita, O. Alekperov, N. Mamedov, *Phys. Status Solidi C* 12 (2015) 826–829.
- [20] R. Paucar, Y.G. Shim, K. Mimura, K. Wakita, O. Alekperov, N. Mamedov, *Phys. Status Solidi C* 14 (2017) 1600214-1–1600214-4.
- [21] N.S. Yuksek, N.M. Gasanly, A. Aydinli, *J. Raman Spectrosc.* 35 (2004) 55–60.
- [22] N.M. Gasanly, A.F. Goncharov, B.M. Dzhavadov, N.N. Melnik, V.I. Tagirov, E.A. Vinogradov, *Phys. Status Solidi B* 92 (1979) K139–K142.
- [23] N.M. Gasanly, A.F. Goncharov, B.M. Dzhavadov, N.N. Melnik, V.I. Tagirov, E.A. Vinogradov, *Phys. Status Solidi B* 97 (1980) 367–377.
- [24] K.R. Allakhverdiev, N.Y. Safarov, M.A. Nizametdinova, N.N. Melnik, A.F. Goncharov, S.I. Subbotin, *Solid State Commun.* 42 (1982) 485–488.
- [25] N.A. Bakhyshov, N.M. Gasanly, B.M. Yavadov, V.I. Tagirov, Sh.M. Efendiev, *Phys. Status Solidi B* 91 (1979) K1–K3.
- [26] A.V. Gomonnai, I. Petryshynets, Yu M. Azhniuk, O.O. Gomonnai, I. Yu Roman, I.I. Turok, A.M. Solomon, R.R. Rosul, D.R.T. Zahn, *J. Cryst. Growth* 367 (2013) 35–41.
- [27] I. Guler, N.M. Gasanly, *Phys. B: Condens. Matter* 406 (2011) 3374–3376.
- [28] I. Guler, N.M. Gasanly, *Appl. Surf. Sci.* 318 (2014) 113–115.
- [29] T.J. Isaacs, J.D. Fekhtner, *J. Solid State Chem.* 14 (1975) 260–263.
- [30] K. Momma, F. Izumi, *J. Appl. Crystallogr.* 44 (2011) 1272–1276.
- [31] A. Dugarte, J. Contreras, G. Díaz de Delgado, M. Delgado, I. Molina-Molina, C. Power, *Rev. LatinAm. Metal. Mater.* 36 (2016) 1–8.
- [32] D.G. Kilday, D. Niles, W. Margaritondo, F. Levy, *Phys. Rev. B* 35 (1987) 660–663.